Opt Quant Electron (2015) 47:901–912
DOI 10.1007/s11082-014-0037-6

# Influence of the surface treatment with low-energy $Ar^+$ plasma on graphene and defected graphene layers

**Teodor Milenov · Ivalina Avramova · Evgenia Valcheva · Savcho Tinchev**

Received: 8 August 2014 / Accepted: 6 October 2014 / Published online: 17 October 2014


**Abstract** Here we present results on the influence of low-energy $Ar^+$ plasma of different duration (from 8 to 60 s) on graphene-containing layers deposited on different surfaces (diamond-like carbon and $SiO_2$) and their subsequent annealing. We used $Ar^+$ plasma with a dose of $10^{15}$ $Ar^+/cm^{-2}$ intended to impact the upper 1 nm thick layer of the treated film. The influence was evaluated by Raman and X-ray photoelectron spectroscopy. It was found that the low-energy $Ar^+$ plasma treatment significantly worsened the quality of graphene and defected graphene even though this was expected. However, a significant self-healing of the modified samples was observed after rapid radiation annealing by 1 kW halogene lamp in vacuum: the FWHM of the 2D band recovers about 90 % of its initial value of 45 $cm^{-1}$, the intensity ratios $I_{2D}/I_G$ and $I_G/I_{D'}$ reach 1.6 and 2.5, respectively. In addition, the final 2D band can be deconvoluted into 6 peaks with FWHM of about 24 $cm^{-1}$ pointing to formation of three-layered graphene.

**Keywords** Graphene · $Ar^+$ plasma · Radiation annealing · Raman spectroscopy · X-ray photoelectron spectroscopy

## 1 Introduction

Graphene is a two-dimensional (2D) material that consists of carbon atoms tightly packed into a honeycomb lattice and is a basic building block for graphitic materials of all other dimen-

T. Milenov (✉) · S. Tinchev
"E. Djakov" Institute of Electronics, Bulgarian Academy of Sciences,
72 Tzarigradsko Chaussee Blvd., 1784 Sofia, Bulgaria
e-mail: teddy@issp.bas.bg

I. Avramova
Institute of General and Inorganic Chemistry, Bulgarian Academy of Sciences,
Acad. G. Bonchev Str., bl. 11, 1113 Sofia, Bulgaria

E. Valcheva
Faculty of Physics, Sofia University, 5 James Bourchier Blvd., 1164 Sofia, Bulgaria

sionalities (see Geim and Novoselov 2007). The carbon atoms are completely $sp^2$ hybridized in graphene. There are many promising applications (field-effect transistors, transparent electrodes, conductive and strengthened composites etc.), determined by the unique properties of graphene. This interest led to development of a lot of different synthesis methods: by the so-called exfoliation (micro-mechanical cleavage of single-crystalline graphite or highly-oriented pyrolytical graphite)—Geim and MacDonald (2007); by chemical vapor deposition (CVD) on metals (Reina et al. 2009; Li et al. 2009; Vo-Van et al. 2011 and semiconductors Berger et al. 2004) etc. The quality of graphene obtained by exfoliation method has the highest perfection, however, the number of exfoliated layers is a practically randomly varying quantity. Graphene synthesized by CVD on metals possesses high local quality (limited to a single graphene flake), however, as the graphene film consists of a lot of graphene flakes (graphene flakes have usually the size of crystal grains of the substrate/metal layer) then the quality of the film in total is worsened due to the concentration of structural defects (grain boundaries etc.). It should also be clearly noted that only CVD deposition methods on metal films have commercial significance. Nevertheless, the application of CVD synthesized graphene in microelectronic production demands removing of the metal foil and further transfer and fixation of the graphene film on an insulating surface. These additional operations create a large number of defects (careers' traps etc.) introducing nonlinearities as higher-order phonon scattering etc. Due to this reason the search for alternative carbon precursors/substrates and experimental conditions that will enable direct deposition of graphene on insulating films continues. A different way for achieving synthesis of graphene directly on insulating surface is proposed by Tinchev (2012) and Tinchev et al. (2013): the authors modify the surface of diamond-like carbon (DLC) films to graphene by low energy $Ar^+$ plasma irradiation and then remove the carbon radicals by thermal annealing. In general, the plasma-based techniques are often used for surface and shallow treatment of materials, especially for application in the electronics/microelectronics. Different experiments of modification of graphene using different ion sources and energies of irradiation: by 30 keV $Ar^+/cm^{-2}$ (Tapasztó et al. 2008), by 500 eV $He^+ - Ne^+$ mixture (Chen et al. 2009), by proton bombardment—$\sim 10^{17} - 10^{19}$ $H^+/cm^2$ (Mathew et al. 2011) etc. were carried out aiming at functionalization of graphene by modification of its charge transport properties. Gokus et al. (2009) used 10 W RF plasma of mixed argon and oxygen (ratio of 2:1) in order to provoke photoluminescence in single-layer graphene. By the way, the authors showed that even 1 s treatment in RF plasma significantly worsened the Raman spectrum of graphene. Mathew et al. (2011) established that the threshold ion dose to introduce an observable damage in mono-layer graphene is $10^{16}$ $H^+/cm^{-2}$.

Here we present results on the influence of low-energy $Ar^+$ plasma on graphene. Our study aims at two main purposes:

(i) we expect that the number of layers in few-layered defected graphene samples (obtained by CVD on (001) Si substrates) will be decreased by short time low-energy $Ar^+$ plasma treatment and
(ii) we present indirect evidence for successful synthesis of graphene and graphene-related phases by CVD and sublimation.

## 2 Experimental

### 2.1 Surface modification of polygraphene and graphene-related phases

We treated two types of specimens by $Ar^+$ plasma: the first type (type A) was polygraphene film (mainly single-layered graphene film consisting of mutually misoriented areas) deposited

on $SiO_2$ and DLC (more details about these films can be found in Ref. Milenov and Avramova 2014), the second type (type B) was a mixed phase (polygraphene mixed with $sp^2/sp^3$ hybridized C:H) deposited on amorphous carbon ($\alpha$-C) and DLC layers (see Ref. Milenov et al. 2014). The surface of all specimens is modified by $Ar^+$ plasma in a simple pulsed bias diode system operating at residual Ar pressure of 0.3 Torr and described earlier in Tinchev et al. (2013). The unipolar voltage amplitude used is 400 V at pulse frequency 66 kHz and pulse length of 10 μs. The $Ar^+$ ion dose is estimated to be $\sim 10^{15}$ $Ar^+/cm^2$ in order to impact the upper 1 nm thick layer of the film—see Refs. Tinchev (2012) and Tinchev et al. (2013). It should be recalled that this level is lower than the threshold for defects' formation established by Mathew et al. (2011) for lighter $H^+$ ions. We use treatment duration of 8, 15, 30 and 60 s in different experiments.

Further on, we annealed a part of the type A specimens in a bilaterally open furnace at 270 °C for 7 min in air atmosphere in order to evaluate the influence of this type of annealing. We used also rapid radiation (RR) annealing suggesting that this process will enhance the recovering and rearrangement of the surface carbon layer in the studied type B specimens. The RRT annealing was performed by radiative heating for 30–60 s in $\sim 3.10^{-6}$ Torr directly in the chamber of a magnetron sputtering system immediately after the surface plasma modification. The source of radiative heating was 1 kW halogen lamp distanced at about 10 cm from the specimens. It was impossible to measure the annealing temperature correctly as the process is quite dynamic and it was carried out in a vacuum chamber. However, we found that the obtained results are reproducible.

### 2.2 Raman spectroscopy measurements

The Raman measurements were carried out at a micro-Raman spectrometer HORIBA Jobin Yvon Labram HR 800 Visible with a He–Ne (633 nm) laser. The laser beam with 0.5 mW power was focused on a spot of about 1 μm in diameter on the studied surfaces, the absolute accuracy being 0.5 $cm^{-1}$ or better.

### 2.3 X-ray photoelectron spectroscopy (XPS)

The X-ray Photoelectron spectra were obtained using non-monochromatized Al $K_\alpha$ (1,486.6 eV) radiation in a VG ESCALAB MK II electron spectrometer under base pressure of $1 \times 10^{-8}$ Pa. The spectrometer resolution was calculated from the $Ag3d_{5/2}$ line with the analyzer transmission energy of 20 eV. The full width at half maximum (FWHM) of this line was 1 eV. The spectrometer was calibrated against the $Au4f_{7/2}$ line (84.0 eV) and the samples' charging was estimated from C1s (285 eV) spectra from natural hydrocarbon contaminations on the surface. The accuracy of the binding energies (BE) measured was 0.2 eV. The photoelectron spectra of C1s and O1s of type A (polygraphene deposited on DLC and $SiO_2$) as well as of type B (mixed graphene-related phases deposited on $\alpha$-C and DLC films) samples were recorded and corrected by subtracting a Shirley-type background and quantified using the peak area and Scofield's photoionization cross-sections.

## 3 Results and discussion

### 3.1 Raman spectroscopy studies

The Raman spectrum is established as a finger print of graphene (Ferrari and Basko 2013) and there are a lot of works that present clear way to distinguish the number of graphene

layers and some particular defects (Ferrari and Basko 2013; Ferrari et al. 2007; Malard et al. 2009; Cong et al. 2011 etc.). Moreover, many authors (see Mathew et al. 2011; Cançado and Jorio 2011; etc.) evaluated defects in graphene caused by ion bombardment by changes in the specific features in its Raman spectrum.

The Raman spectrum of our as-deposited layers (lower traces in Figs. 1, 2) contains the main features of the Raman spectrum of graphene (Ferrari and Basko 2013; Ferrari et al. 2007): the G-peak (the only first-order Raman band in graphene possessing $E_{2g}$- symmetry) and the 2D band (the overtone of D-band)—see Ferrari et al. (2007). The shape and position of the 2D band are found to enable the identification of mono-, bi-, three- and four-layered graphene (Ferrari et al. 2007; Malard 2009; Cong et al. 2011). We observed also the D and the D′ band that are expected to appear in defected-graphene samples: the D-peak is due to breathing-like modes of C hexagonal rings (corresponding to transverse optical phonons near the K point) and requires a defect for its activation via an intervalley double-resonance Raman process (Thomsen and Reich 2000) while the peak, denoted as D′ (at about 1,610 $cm^{-1}$ for 633 nm excitation wavelength) is very similar to D and occurs via an intravaley double-resonance process in the presence of defects (Nemanich and Solin 1979; Malard et al. 2009). The peak intensities (peak heights) of the features D, G, D′ and 2D ($I_D$, $I_G$, $I_{D'}$ and $I_{2D}$) as well as the full width at half maximum (FWHM) of 2D band in different samples are presented in Tables 1 and 2. Several combination bands could also be distinguished in our Raman spectra (Figs. 1, 2, 3): G* (due to iTA+LA i.e. in-plane transverse and longitudinal acoustical phonons), (D+D′), and the $B_1$ ((iTO+LA) and $B_2$ (iLO+LA)) combination bands, respectively (Cong et al. 2011 as well as 2D′ overtone of DD′) could also be distinguished in our Raman spectra (Figs. 1, 2, 3). The HC-marked feature that appears at about 1,135 $cm^{-1}$ is attributed to the presence of ($sp^2 + sp^3$)-C:H species (Michaelson and Hoffman 2006).

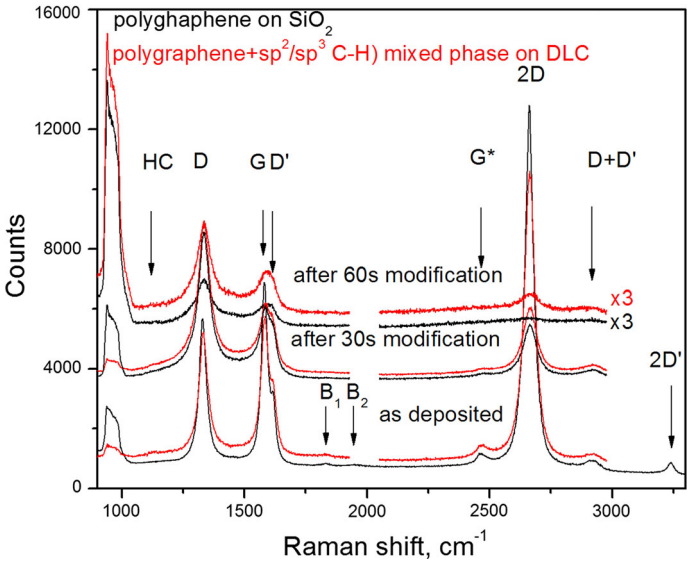


**Fig. 1** (color online) Raman spectra of single-layered polygraphene on $SiO_2$ (*red traces*) and 2–4 layered polygraphene and ($sp^2/sp^3$ C)-H species mixed phases deposited on DLC (*green traces*): as deposited (*lower traces*), after 30 s $Ar^+$ surface modification (*middle traces*) and after 60 s $Ar^+$ surface modification (*upper traces*)

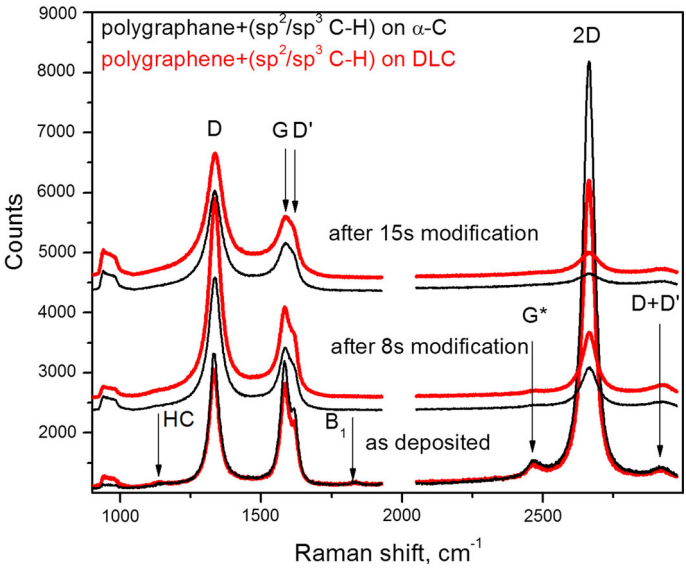


**Fig. 2** (color online) Raman spectra of mixed phase of polygraphene and ($sp^2/sp^3$ C)-H species (*black traces*) on ($\alpha$-C) and the same mixed phase as 2–4 layered carbon film on DLC (*red traces*) layers: as deposited (*lower traces*), after 8 s $Ar^+$ surface modification (*middle traces*) and after 15 s $Ar^+$ surface modification (*upper traces*)

**Table 1** The summarized results of surface modification of polygraphene films deposited by sublimation on $SiO_2$ and DLC

| Surface treatment of polygraphene | FWHM of 2D, $cm^{-1}$ | | $I_{2D}/I_G$ | | $I_G/I_{D'}$ | |
|---|---|---|---|---|---|---|
| | On $SiO_2$ | On DLC | On $SiO_2$ | On DLC | On $SiO_2$ | On DLC |
| As deposited | 41 | 56 | 2.08 | 2.22 | 3.76 | 2.85 |
| After 30 s $Ar^+$ treatment | 90 | 100 | 0.94 | 1.16 | 1.71 | 1.76 |
| After 60 s $Ar^+$ treatment and annealing at 270 °C in air for 7 min | – | – | – | – | 0.9 | 1.47 |

The results are averaged and the deviation of different particular values does not exceed ±5 %

**Table 2** The summarized results of surface modification and RT annealing of mixed polygraphene/($sp^2+sp^3$)-C:H phase deposited on $\alpha$-C and DLC surfaces

| Surface treatment | FWHM of 2D, $cm^{-1}$ | | $I_{2D}/I_G$ | | $I_G/I_{D'}$ | |
|---|---|---|---|---|---|---|
| | $\alpha$-C | DLC | $\alpha$-C | DLC | $\alpha$-C | DLC |
| As deposited | 43 | 54 | 3.48 | 3.18 | 2.05 | 2.09 |
| After 8 s $Ar^+$ plasma treatment | 80 | 90 | 0.71 | 0.75 | 1.3 | 1.4 |
| After RT annealing for 45 s | 50 | 50 | 1.33 | 1.16 | 2.16 | 2.02 |
| After 15 s $Ar^+$ plasma treatment | 100 | 120 | 0.35 | 0.48 | 1.42 | 1.70 |
| After RT annealing for 45 s | 54 | 56 | 0.78 | 1.0 | 1.98 | 2.71 |

The results are averaged and the deviation of different particular values does not exceed ±5 %

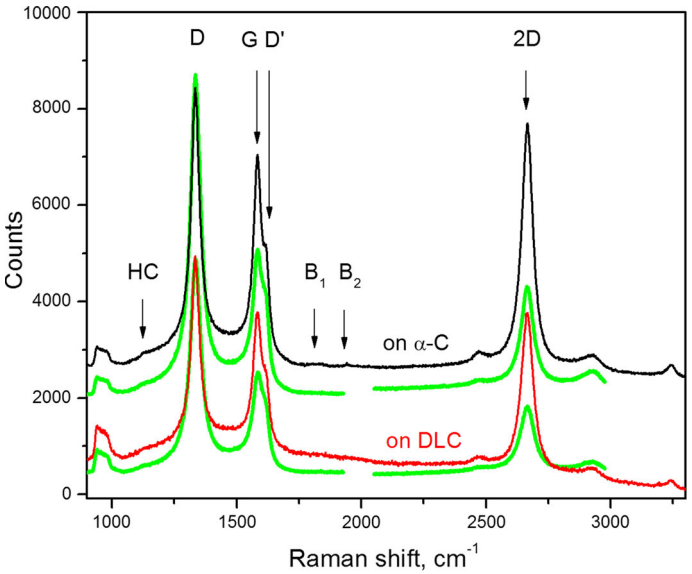


**Fig. 3** (color online) Raman spectra of polygraphene and ($sp^2/sp^3$ C)-H species on ($\alpha$-C) and DLC layers after 8 s $Ar^+$ surface modification (*green lower traces*) and after RR annealing (*red* and *black traces*, respectively)

The surface treatment of A-type specimens (polygraphene films deposited on $SiO_2$ surface) leads to a significant worsening of the layers' quality: the spectrum (after $Ar^+$ treatment) is dominated by the D- band and the intensity of 2D band decreases more than 10 times after 30 s plasma treatment duration and 7 min thermal annealing at 270 °C in air atmosphere. The layer practically disappears after 60 s plasma treatment and 7 min thermal annealing in air atmosphere. The position of 2D band is weakly blueshifted with about 5–10 $cm^{-1}$. The intensity of the D′ band increases with the irradiation time. The influence of the same treatment on few-layer polygraphene on DLC is similar. The Raman spectra are shown in Fig. 1 and the results are summarized in Table 1.

The results of $Ar^+$ surface treatment of the B-type substrates (mixed polygraphene/($sp^2 + sp^3$)-C:H phase deposited on $\alpha$- C and DLC surfaces) are similar to those for A-type specimens. The D-band dominates the Raman spectrum. The intensity of 2D band remains comparable to that of G-band (see Fig. 2; Table 2) due to the lower exposure time (8 and 15 s) but it is weakly blueshifted by about 5 $cm^{-1}$. The intensity ratios $I_{2D}/I_G$ and $I_G/I_D$ decrease with increasing exposure time (Fig. 2; Table 2). The performed RR annealing significantly recovers the initial structure of the layers as we observe attributes of few-layer defected graphene Raman spectrum: the 2D FWHM is ~50 $cm^{-1}$, the intensity ratios $I_{2D}/I_G$ and $I_G/I_{D'}$ are 1.33 and 2.16, respectively and the $B_1$ and $B_2$ combination bands (see Cong et al. 2011) appear distinguishable—Figs. 3, 4, 5 and Table 2. The D band remains the dominating feature after RR annealing. We used curve fitting in order to resolve the complex structure of the 2D and (G+D′) bands. The example results of 2D band deconvolution from the Raman spectrum of type B specimen treated with $Ar^+$ plasma for 8 s and further RR annealed are shown in Fig. 5a, b. It is well known that the number of peaks constituting 2D band increases with increasing number of graphene layers. Most researchers use for the deconvolution procedure peaks with FWHM of ~24 $cm^{-1}$ and it is clearly established that the 2D band of bi-layer (AB-stacked) graphene can be deconvoluted into 4 peaks (see Ferrari et al. 2007;

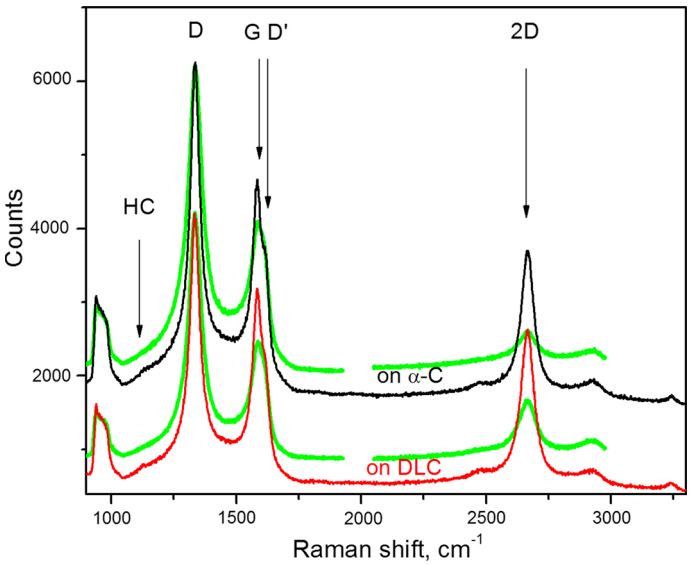


**Fig. 4** (color online) Raman spectra of polygraphene and ($sp^2/sp^3$ C)-H species on ($\alpha$-C) and DLC layers after 15 s $Ar^+$ surface modification (*green upper traces*) and after RR annealing (*red* and *black traces*, respectively)

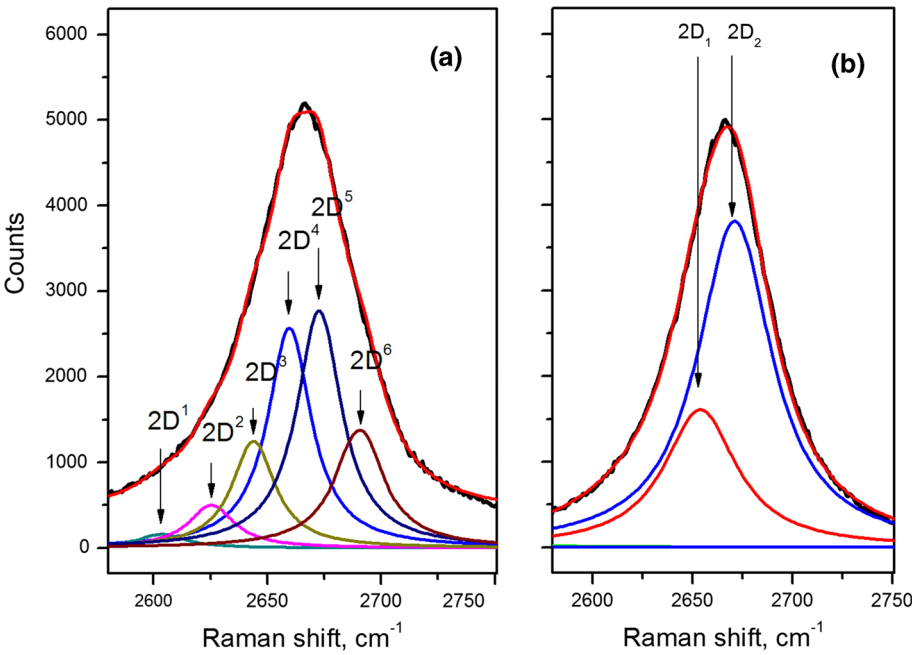


**Fig. 5** (color online) Deconvolution of the 2D band of the Raman spectra of mixed polygraphene and ($sp^2/sp^3$ C)-H species on ($\alpha$-C) layer after 8 s $Ar^+$ surface modification and RR annealing. **a** Deconvolution of the 2D band into 6 Lorentzians (FWHM ~24 $cm^{-1}$): $D^1$, $D^2$, $D^3$, $D^4$, $D^5$ and $D^6$; **b** deconvolution of the 2D band into 2 Lorentzians (FWHM ~35–40 $cm^{-1}$): $D_1$ and $D_2$

Malard et al. 2009; Malard 2009). It is also established that that 2D band of three-layered graphene (Malard et al. 2009) can be deconvoluted into 6 peaks with higher intensity and the rest 9 peaks are indistinguishable due their low intensity (when the Raman spectrum is excited by 514.5 nm as well as by 568.7 nm laser wavelength). We successfully deconvoluted the 2D band into 6 peaks (FWHM $\sim$24 cm$^{-1}$)—see Fig. 5 a which implies that we have three-layered polygraphene in this case. On the other hand, we show that the same 2D band can be deconvoluted in another way: into two bands ($D_1$ and $D_2$ with FWHM of $\sim$40 cm$^{-1}$) following Ni et al. (2008). These authors found that the 2D band of graphene of graphite substrate (centered at about 2,660 cm$^{-1}$) can be deconvoluted into two bands with FWHM of $\sim$35–40 cm$^{-1}$. However, we concluded that there is a three-layered graphene as Ni et al. (2008) related the broadening and blue-shift of the 2D band to the influence of the substrate (graphite in their case) while we have defected graphene on amorphous carbon substrate.

### 3.2 XPS studies

In order to clarify the influence of $Ar^+$ plasma treatment and thermal/rapid radiation annealing we studied all specimens by XPS. It should be recalled that the measured XPS spectra are integral, i.e. we collect signal from the entire surface of specimens. We used curve fitting to resolve the complex peaks in the spectral range 275–295 eV (the area around C1s core level).

The fitted C1s photoelectron spectra of untreated samples, those treated with $Ar^+$ plasma for 30 s as well as those treated in $Ar^+$ plasma for 60 s and thermally annealed at 270 °C for 7 min (A-type specimens) reveal existence of $sp^2$- and $sp^3$-bonded carbon (around 284.0–284.4 and 284.7–284.9 eV, respectively) as well as C–O (at about 286.5 eV) and C=O (at about 288 eV) functional groups on the surface of the specimens—Fig. 6a–c. Few important differences among XPS spectra in Fig. 6a–c should be remarked:

- the photoelectron peak of $sp^2$-hybridized carbon is moderately downshifted (from the typical value for graphene of 284.4 eV (see Becerril et al. 2008) to about 284.0 eV—value typical for amorphous carbon (see Lascovich et al. 1991; Díaz et al. 1996);
- the photoelectron peak of $sp^3$-hybridized carbon preserves its value of 284.8 eV—a value typical for diamond (Morar et al. 1986; Johnson et al. 2007; Wilson et al. 2001) in all A-type specimens;
- the $sp^2C/sp^3C$ ratio varies from 10/2.0 in untreated samples to 10/8.7 and 10/9.5 after 30 s $Ar^+$ plasma treatment and 60 s treatment with subsequent annealing, respectively;
- the C–O functional groups are of significantly higher content then the C=O ones in the untreated A-type specimens while the opposite situation (clear domination of C=O groups) is observed in those treated for 60 s in $Ar^+$ plasma and thermally annealed. The C–O to C=O groups ratio in the A-type specimen treated for 30 s in $Ar^+$ plasma is 1:2;
- the peak between 290–292 eV corresponding to the $\pi - \pi^*$ bond typical for $sp^2$-hybridization (Svensson et al. 1988; Bradshaw et al. 1974) appears in the untreated samples only.

The fitted C1s photoelectron spectra of untreated B-type specimens, those treated in $Ar^+$ plasma for 8 and 15 s and further rapid radiation annealed for 45 s (Fig. 7a–c) are similar to the above described spectra. The specific differences among the XPS spectra shown in Fig. 7a–c can be summarized as follows:

- the photoelectron peak of $sp^2$-hybridized carbon is moderately downshifted (from the typical value for graphene of 284.4 eV) to about 284.1 eV—a value similar to that typical for amorphous carbon in the sample treated for 15 s and RRT annealed and nearly

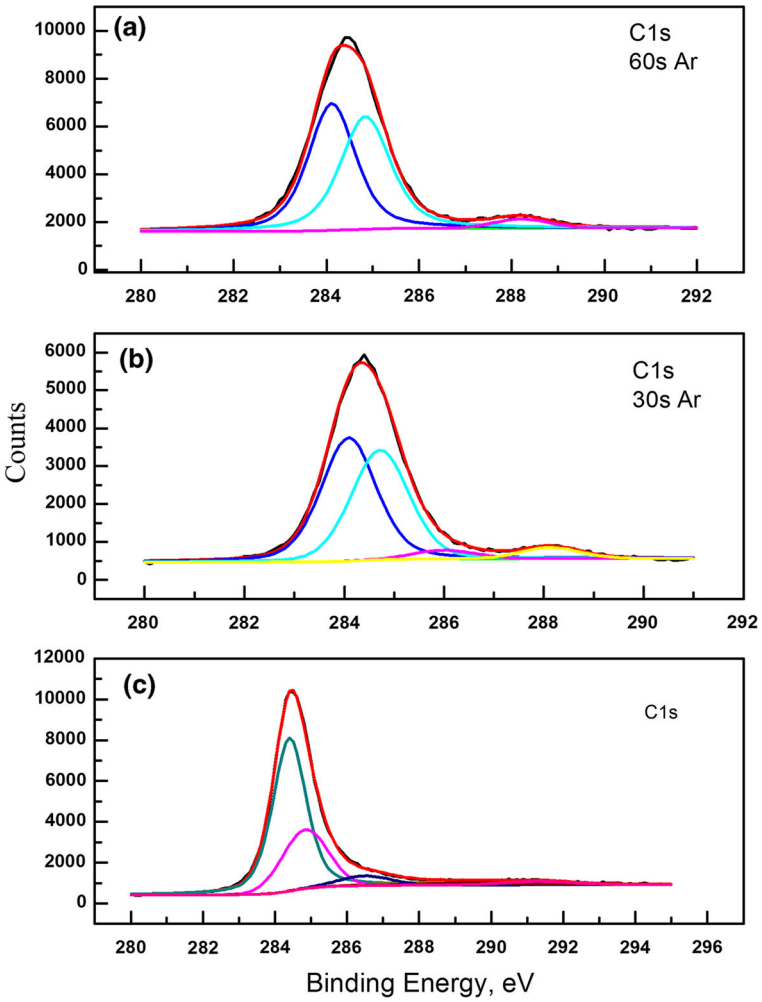


**Fig. 6** (color online) **a** Deconvolution of C1s photoelectron line for the pristine sample of polygraphene deposited by sublimation of HOPG; **b** deconvolution of C1s photoelectron line for the same sample after 30 s treatment by $Ar^+$ plasma; **c** deconvolution of C1s photoelectron line for the same sample after 60 s treatment by $Ar^+$ plasma and 7 min thermal annealing (270 °C in air atmosphere)

preserves its value (it appears at about 284.3 eV) in the sample treated for 8 s and RRT annealed;

- the photoelectron peak of $sp^3$-hybridized carbon preserves its value of 284.8–284.9 eV typical for diamond in all B-type samples;
- the $sp^2C/sp^3C$ ratio varies from 10/2.5 in untreated samples to 10/5 and 10/8.6 in specimens treated 8 and 15 s with $Ar^+$ plasma and further RRT annealed, respectively;
- there are significantly more C–O functional groups then C=O groups in the pristine B-type specimen while the opposite situation (pronounced domination of C=O groups) is observed in the B-type specimen treated for 15 s with $Ar^+$ plasma and RRT annealed. The contents' ratio of C-O to C=O groups in the B-type specimen treated for 8 s with $Ar^+$ plasma and RRT annealed is 2:1;

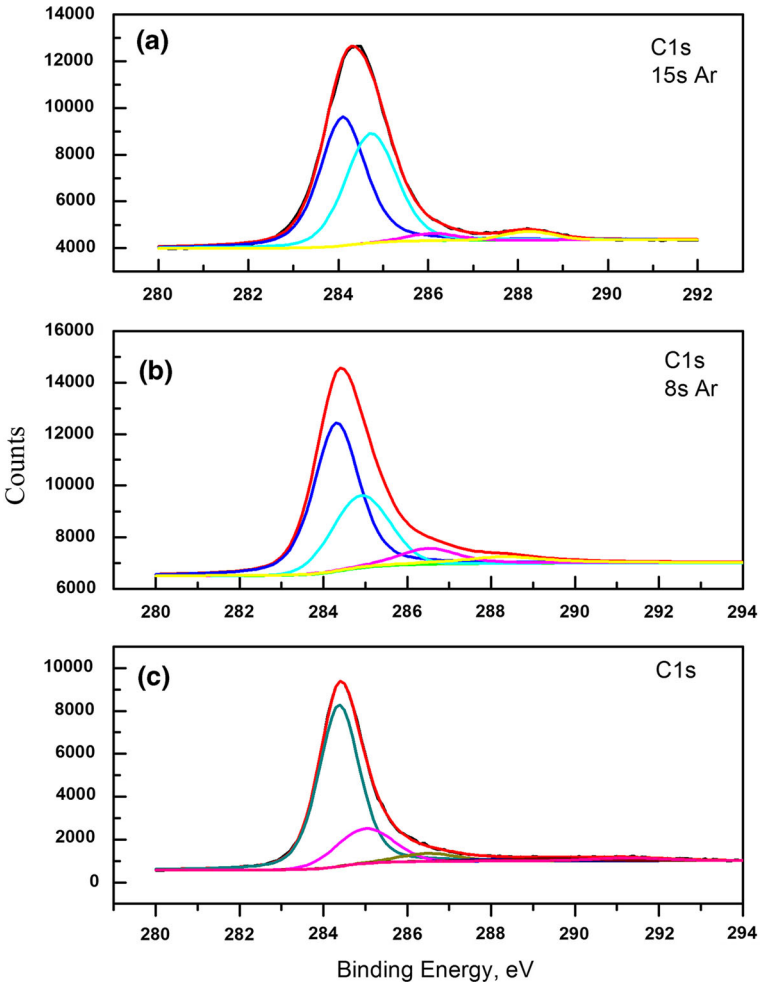


**Fig. 7** (color online) **a** Deconvolution of C1s photoelectron line for the pristine sample of mixed phase of polygraphene and ($sp^2$ /$sp^3$ C)-H species; **b** deconvolution of C1s photoelectron line for the same sample after 8 s treatment by $Ar^+$ plasma and 45 s RR annealing; **c** deconvolution of C1s photoelectron line for the same sample after 15 s treatment by $Ar^+$ plasma and 45 s RR annealing

– the peak between 290–292 eV corresponding to the $\pi - \pi^*$ bond typical for $sp^2$-hybridization is distinguishable in the pristine B-type sample only.

The XPS results confirm in general those of the Raman spectroscopy studies: the low-energy $Ar^+$ plasma treatment (below the damage threshold of $10^{16}$ ions/$cm^{-2}$) worsenes the quality of polygraphene layers even after 8 s treatment. The Ar plasma influences the surface $sp^2$-C framework by dangling of the C–C bonds and formation of carbon vacancies. It seems also that the $sp^3$-C species remain relatively unaffected by the plasma treatment. Moreover, we establish an increased $sp^3$-C content in all plasma-treated samples accompanied with increased presence of C=O functional groups after annealing.

We also found clear evidence for recovering of defected graphene layers deposited on amorphous carbon layers: the Raman spectrum of the layer becomes similar to the initial

one after rapid radiation annealing by 1 kW halogen lamp for 45 s. We suggest that the $Ar^+$ irradiation (even for 8 s) drives out C atoms from the polygraphene layer and the intermediate $\alpha$-C films creating surface roughness. Further on, we suggest that a rearrangement of carbon atoms takes place during the RT annealing. Therefore, we ascribe this recovering to the pronounced self-healing ability of graphene established by Barreiro et al. (2013).

## 4 Conclusions

Finally, we can draw several conclusions. Regarding to the surface modification of polygraphene and graphene-related phases: (i) the predominantly single-layered polygraphene sublimated on $SiO_2$ is seriously damaged after 30 s and is practically destroyed after 60 s irradiation with $Ar^+$ plasma; (ii) the quality of predominantly single-layered mixed phase of polygraphene and $sp^2/sp^3$ bonded C–H species deposited by CVD on (001) Si substrates with a-C interlayer is also significantly worsened even after 8 and 15 s irradiation with $Ar^+$ plasma; (iii) a similar effect is observed after the treatment of such layers deposited on DLC layers. These experiments yield an indirect indication that the synthesized carbon films contain predominantly single-layered phases. The observed self-healing of mixed polygraphene/($sp^2+sp^3$)-C:H phase deposited on $\alpha$-C and DLC surfaces after RT annealing is most probably due to diffusion of carbon from the $\alpha$-C intermediate layer between the polygraphene and Si surfaces and rearrangement of the surface layer.

**Acknowledgments** The authors gratefully acknowledge support from MPNS COST ACTION MP1204-TERA-MIR Radiation: Materials, Generation, Detection and Applications.

## References

Barreiro, A., Boerrnert, F., Avdoshenko, S.M., Rellinghaus, B., Cuniberti, G., Ruemmeli, M.H., Vandersypen, L.M.K.: Understanding the catalyst-free transformation of amorphous carbon into graphene by current-induced annealing. Sci. Rep. **3**, 1115–1–6 (2013). doi:10.1038/srep01115

Becerril, H.A., Mao, J., Liu, Z., Stoltenberg, R.M., Bao, Z., Chen, Y.: Evaluation of solution-processed reduced graphene oxide films as transparent conductors. ACS Nano **2**, 463–470 (2008)

Berger, C., Song, Z., Li, T., Li, X., Ogbazghi, A.Y., Feng, R., Dai, Z., Marchenko, A.N., Conrad, E.H., First, P.N.: Ultrathin epitaxial graphite: 2D electron gas properties and a route toward graphene-based nanoelectronics. J. Phys. Chem. **108**, 19912–19916 (2004)

Bradshaw, A.M., Cederbaum, S.L., Domcke, W., Krause, U.: Plasmon coupling to core hole excitations in carbon. J. Phys. C Solid State 7, 4503–4512 (1974)

Cançado, L.G., Jorio, A., Ferreira, E.H.M., Stavale, F., Achete, C.A., Capaz, R.B., Moutinho, M.V.O., Lombardo, A., Kulmala, T.S., Ferrari, A.C.: Quantifying defects in graphene via Raman spectroscopy at different excitation energies. Nano Lett. **11**, 3190–3196 (2011)

Chen, J.H., Cullen, W.G., Williams, E.D., Fuhrer, M.F.: Defect scattering in graphene. Phys. Rev. Lett. **102**, 236805–1–4 (2009)

Cong, C., Yu, T., Saito, R., Dresselhaus, G.F., Dresselhaus, M.S.: Second-order overtone and combination Raman modes of graphene layers in the range of 1690–2150 $cm^{-1}$. ACS Nano **5**, 1600–1605 (2011)

Díaz, J., Paolicelli, G., Ferrer, S., Comin, F.: Separation of the $sp^3$ and $sp^2$ components in the C1s photoemission spectra of amorphous carbon films. Phys. Rev. B **54**, 8064–8069 (1996)

Ferrari, A.C., Basko, D.M.: Raman spectroscopy as a versatile tool for studying the properties of graphene. Nat. Nanotechnol. **8**, 235–246 (2013)

Ferrari, A.C., Meyer, J.C., Scardaci, V., Casiraghi, C., Lazzeri, M., Mauri, F., Piscanec, S., Jiang, D., Novoselov, K.S., Roth, S., Geim, A.K.: Raman spectrum of graphene and graphene layers. Phys. Rev. Lett. **97**, 187401–187404 (2007)

Geim, A.K., Novoselov, K.S.: The rise of graphene. Nat. Mater. **6**, 183–191 (2007)

Geim, A.K., MacDonald, A.H.: Graphene: exploring carbon flatland. Phys. Today **60**, 35–41 (2007)

Gokus, T., Nair, R.R., Bonetti, A., Böhmler, M., Lombardo, A., Novoselov, K.S., Geim, A.K., Ferrari, A.C., Hartschuh, A.: Making graphene luminescent by oxygen plasma treatment. ACS Nano **3**, 3963–3968 (2009)

Johnson, J.A., Holland, D., Woodford, J.B., Zinovev, A., Gee, I.A., Eryilmaz, O.L., Erdemir, A.: Top surface characterization of a near frictionless carbon film. Diam. Relat. Mater. **16**, 209–215 (2007)

Lascovich, J.C., Giorgi, R., Scaglione, S.: Evaluation of the $sp^2/sp^3$ ratio in amorphous carbon structure by XPS and XAES. Appl. Surf. Sci. **47**, 17–21 (1991)

Li, X., Cai, W., An, J., Kim, S., Nah, J., Yang, D., Piner, R., Velamakanni, A., Jung, I., Tutuc, E., Banerjee, S.K., Colombo, L., Ruoff, R.S.: Large-area synthesis of high-quality and uniform graphene films on copper foils. Science **324**, 1312–1314 (2009)

Malard, L.M., Pimenta, M.A., Dresselhaus, G.F., Dresselhaus, M.S.: Raman spectroscopy in graphene. Phys. Rep. **473**, 51–87 (2009)

Malard, L.M., Guimarães, M.H.D., Mafra, D.L., Mazzoni, M.S.C., Jorio, A.: Group-theory analysis of electrons and phonons in $N$-layer graphene systems. Phys. Rev. B **79**, 125426-1–125426-8 (2009)

Mathew, S., Chan, T.K., Zhan, D., Gopinadhan, K., Barman, A.R., Breese, M.B.H., Dhar, S., Shen, Z.X., Venkatesan, T., Thong, J.T.L.: Mega-electron-volt proton irradiation on supported and suspended graphene: a Raman spectroscopic layer dependent study. J. Appl. Phys. **110**, 084309–1–9 (2011)

Michaelson, Sh, Hoffman, A.: Hydrogen bonding, content and thermal stability in nano-diamond films. Diam. Relat. Mater. **15**, 486–497 (2006)

Milenov T.I., Avramova I.: Deposition of graphene by sublimation of pyrolitic carbon, Opt. Quantum Electron., (2014). doi:10.1007/s11082-014-0015-z

Milenov, T.I., Avramova, I., Avdeev, G.V.: CVD of graphene-related phases by thermal decomposition of acetone on different substrates. Thin Solid Films—submitted (2014)

Morar, J.F., Himpsel, F.J., Hollinger, G., Jordan, J.L., Hughes, G., McFeely, F.R.: Carbon 1s excitation studies of diamond (111). I. Surface core levels. Phys. Rev. B **33**, 1340–1345 (1986)

Nemanich, R.J., Solin, S.A.: First- and second-order Raman scattering from finite-size crystals of graphite. Phys. Rev. B **20**, 392–401 (1979)

Ni, Z., Wang, Y., Yu, T., Shen, Z.: Raman spectroscopy and imaging of graphene. Nano Res. **1**, 273–291 (2008)

Reina, A., Jia, X., Ho, J., Nezich, D., Son, H., Bulovic, V., Dresselhaus, M.S., Kong, J.: Large area, few-layer graphene films on arbitrary substrates by chemical vapor deposition. Nano Lett. **9**, 30–35 (2009)

Svensson S, Eriksson B, Maartensson N, Wendin G, Gelius U. Electron shake-up and correlation satellites and continuum shake-off distributions in x-ray photoelectron spectra of the rare gas atoms, J. Electron Spectrosc. Relat. Phenom. 47, 327–384 (1988)

Tapasztó, L., Dobrik, G., Nemes-Incze, P., Vertesy, G., Lambin, P.H., Biró, L.P.: Tuning the electronic structure of graphene by ion irradiation. Phys. Rev. B **78**, 233407–1–4 (2008)

Thomsen, C., Reich, S.: Double resonant Raman scattering in graphite. Phys. Rev. Lett. **85**, 5214–5217 (2000)

Tinchev, S.S.: Surface modification of diamond-like carbon films to graphene under low energy ion beam irradiation. Appl. Surf. Sci. **258**, 2931–2934 (2012)

Tinchev, S.S., Valcheva, E., Petrova, E.: Low temperature crystallization of diamond-like carbon films to graphene. Appl. Surf. Sci. **280**, 512–517 (2013)

Vo-Van, C., Kimouche, A., Reserbat-Plantey, A., Fruchart, O., Bayle-Guillemaud, P., Bendiab, N., Coraux, J.: Epitaxial graphene prepared by chemical vapor deposition on single crystal thin iridium films on sapphire. Appl. Phys. Lett. **98**, 181903–1–4 (2011)

Wilson, J.I.B., Walton, J.S., Beamson, G.: Analysis of chemical vapour deposited diamond films by X-ray photoelectron spectroscopy. J. Electron Spectrosc. Relat. Phenom. **121**, 183–201 (2001)